

# ELECTROMECHANICAL INTERACTION IN ECCENTRIC-ROTOR CAGE INDUCTION MACHINE EQUIPPED WITH A SELF-BEARING FORCE ACTUATOR

**Antti Laiho**

VTT Technical Research Centre of Finland, FI-02044 VTT, Finland  
antti.laiho@vtt.fi

**Kari Tammi**

VTT Technical Research Centre of Finland, FI-02044 VTT, Finland  
kari.tammi@vtt.fi

**Juha Orivuori**

Helsinki University of Technology, Control Engineering Laboratory, FI-02015 TKK, Finland  
juha.orivuori@tkk.fi

**Anssi Sinervo**

Helsinki University of Technology, Laboratory of Electromechanics, FI-02015 TKK, Finland  
asinervo@cc.hut.fi

**Kai Zenger**

Helsinki University of Technology, Control Engineering Laboratory, FI-02015 TKK, Finland  
kai.zenger@tkk.fi

**Antero Arkkio**

Helsinki University of Technology, Laboratory of Electromechanics, FI-02015 TKK, Finland  
antero.arkkio@tkk.fi

## **ABSTRACT**

In this paper, flexural rotor vibration in a two-pole cage induction machine equipped with a built-in force actuator is examined. The built-in force actuator is based on the self-bearing machine technology in

which a supplementary winding is placed in the machine for force production. The built-in force actuator enables active vibration control, but also it enables excitation of the machine for purposes of condition monitoring, for instance. A low-order parametric model is derived for the actuator-rotor system. In the

model, the arbitrary eccentric rotor motion is coupled with the voltage-flux equations for the eccentric rotor cage and supplementary winding. Furthermore, based on frequency-domain system identification, an adaptive control method is examined for compensating rotor rotation harmonic vibration components. Experimental results are given for a two-pole cage induction motor. The main contribution of the article is to couple eccentric rotor motion, the built-in force actuator and the mechanical rotor model to obtain a low-order parametric model of the actuator-rotor system which can be applied to control design for rotor vibration suppression.

## INTRODUCTION

In this paper, eccentric rotor motion and flexural rotor vibration in a cage induction machine equipped with a built-in force actuator is examined. When the rotor is displaced from the stator center, the air-gap magnetic field is distorted and a net force, referred to as unbalanced magnetic pull (UMP) [1], is exerted on the rotor. As a result, rotordynamic characteristics of the machine change. In its extreme, the flexural rotor bending modes may couple with the electromechanical system and induce rotordynamic instability.

We consider an induction machine equipped with a built-in force actuator which is based on the self-bearing machine technology [2, 3] in which a supplementary three-phase winding is distributed to the stator slots. When current is fed to the supplementary winding, the air-gap field is distorted and a force is exerted on the rotor.

In this paper, a low-order parametric model is derived for the actuator-rotor system. In the model, the arbitrary eccentric rotor motion is coupled with the voltage-flux equations for the eccentric rotor cage and supplementary winding [4, 5]. We present experimental results in which a test motor with extended rotor shaft is equipped with the built-in force actuator. The low-order model is identified by using vibration measurement data from the test machine. Furthermore, the built-in force actuator is applied for flexural rotor vibration attenuation. Indeed, low-frequency harmonic rotor rotation harmonics are compensated

by using an adaptive control algorithm [6].

The main contribution of the paper is to couple eccentric rotor motion, the built-in force actuator and the mechanical rotor model to obtain a low-order parametric model of the system. The methodology presented provides enhanced means of model-based control design for flexural rotor vibration control.

## MODELLING

In the following, we deduce a parametric model for a two-pole cage induction machine equipped with a supplementary four-pole winding (referred to as 'control winding') for force production. In the stator coordinates, by using the space vector formalism, we write the voltage-flux equations [7]

$$\hat{U}_c = R_{c,2}\hat{i}_{c,2} + \frac{d\hat{\psi}_{c,2}}{dt} \quad (1)$$

$$0 = R_{r,2}\hat{i}_{r,2} + \frac{d\hat{\psi}_{r,2}}{dt} - 2j\omega_m\hat{\psi}_{r,2} \quad (2)$$

where  $\hat{U}_c$  is (space vector of) the voltage supplied to the control winding,  $R_{c,2}$  the control winding resistance,  $\hat{i}_{c,2}$  the current in the control winding,  $R_{r,2}$  the rotor cage four-pole harmonic resistance,  $\omega_m$  the rotor rotation angular frequency. The subindex '2' refers to pole-pairs. The four-pole flux through the control winding and the rotor cage,  $\hat{\psi}_{c,2}$  and  $\hat{\psi}_{r,2}$  respectively, are given by

$$\hat{\psi}_{c,2} = L_{c,2}\hat{i}_{c,2} + M_{r,c,2}\hat{i}_{r,2} + \frac{L_{c,\epsilon,2}}{2\mu_0}\hat{B}_1z_r \quad (3)$$

$$\hat{\psi}_{r,2} = L_{r,2}\hat{i}_{r,2} + M_{r,c,2}\hat{i}_{c,2} + \frac{L_{r,\epsilon,2}}{2\mu_0}\hat{B}_1z_r \quad (4)$$

where  $L_{c,2}$  denotes the control winding inductance,  $M_{r,c,2}$  the mutual inductance between the rotor cage and the control winding,  $L_{r,2}$  the rotor cage inductance and  $z_r$  the rotor center displacement measured from the stator bore center. Under constant-flux operational conditions, the two-pole flux is given by

$$\hat{B}_1 = \underline{B}_1 e^{j\omega_1 t} \quad (5)$$

where  $\underline{B}_1$  is a complex constant and  $\omega_1$  is the supply frequency of the torque-producing two-pole stator

winding. In Eqs. (3) and (4), we have used the model for eccentric rotor cage introduced by Holopainen *et al.* [4]. The model presented by Holopainen *et al.* includes the inductance  $L_{r,\epsilon,2}$  induced by the eccentric rotor motion and here the inductance term  $L_{c,\epsilon,2}$  was added due to the control winding.

The force exerted on the rotor is calculated from the Maxwell stress tensor yielding

$$\underline{f}_c = \frac{\pi d_r l_r}{8\mu_0 \delta_0} |\underline{B}_1|^2 \underline{z}_r + \frac{\pi d_r l_r}{4\delta_0} \hat{B}_1^* (k_{r,2} \hat{l}_{r,2} + k_{c,2} \hat{l}_{c,2}) \quad (6)$$

where  $d_r$  is the rotor core diameter,  $l_r$  the rotor core axial length,  $\mu_0 = 4\pi \cdot 10^{-7}$  N/A<sup>2</sup> permeability of vacuum,  $\delta_0$  the radial air-gap and  $k_{r,2}$  and  $k_{c,2}$  coupling factors.

The mechanical Jeffcott rotor model in the stator coordinate system is given by

$$\ddot{z}_r + 2\xi\omega_0\dot{z}_r + \omega_0^2 z_r = (\underline{f}_c + \underline{f}_{ex})/m. \quad (7)$$

where  $\omega_0$  is the first rotor bending natural frequency,  $\xi$  the modal damping and  $m$  the rotor mass. Furthermore, the external excitation force  $\underline{f}_{ex}$  is dominated by the rotor rotation harmonics.

By substituting Eq. (6) to Eq. (7) with Eq. (5) we obtain a model with periodically time-varying coefficients. However, by introducing

$$\begin{aligned} \hat{U}_{c,0} &= \hat{U}_c e^{-j\omega_1 t} \\ \hat{l}_{c,2,0} &= \hat{l}_{c,2} e^{-j\omega_1 t} \\ \hat{l}_{r,2,0} &= \hat{l}_{r,2} e^{-j\omega_1 t} \end{aligned}$$

we obtain a linear time-invariant (LTI) model for the actuator-rotor system. The input of the system is the voltage  $\hat{U}_{c,0}$  supplied to the control winding with the disturbance force  $\underline{f}_{ex}$ . The states of the system are the currents in the control winding  $\hat{l}_{c,2,0}$  and the rotor cage  $\hat{l}_{r,2,0}$  with rotor radial position  $\underline{z}_r$  being the measurable output.

## ROTOR VIBRATION CONTROL

For the actuator-rotor system, the convergent control (CC) algorithm [6] was used for attenuation of vibration originated from periodic excitations. The

algorithm operates on the frequency-domain with the Fourier coefficients  $\hat{v}$  of the control input  $v = (\text{Re}(\hat{U}_{c,0}), \text{Im}(\hat{U}_{c,0}))^T$  at excitation frequency  $\omega$  given by the adaptive law

$$\hat{v}_c(k+1) = \gamma \hat{v}_c(k) - \alpha \mathcal{H}(j\omega)^\dagger \hat{u}_{rc}(k) \quad (8)$$

where  $\hat{u}_{rc}$  is the Fourier coefficient of the rotor displacement  $u_{rc} = (\text{Re}(z_r), \text{Im}(z_r))^T$  at  $\omega$ ,  $\mathcal{H}(j\omega)$  is (an estimate of) the frequency-response of the actuator-rotor system at  $\omega$ , ' $\dagger$ ' denotes the matrix pseudo-inverse operator and  $0 < \gamma \leq 1$ ,  $\alpha > 0$  are parameters related to the convergence of the algorithm. If the excitation is composed of several frequencies CC algorithm operates on each excitation frequency in a separate feedforward adaptation loop.

## EXPERIMENTAL SET-UP

A two-pole 30kW cage induction motor (see Fig. 1) was used in experiments. The motor was equipped with an extended rotor shaft (length 1560 mm, total weight with rotor stack 55.8 kg) with first rotor bending mode being 37.5 Hz. The control winding for force production was a four-pole three-phase winding with 20 turns in each phase. Displacement transducers were attached at the driving end of the machine close to the end-shield. During the experiments, the machine was run without load at 17.2 Hz (rated 50 Hz) rotation frequency and 79.0 V / 14.9 A (rated 380 V / 20 A) torque-producing two-pole winding supply.

The online signal processing was performed by using dSpace system operating in SIMULINK environment by using MATLAB Real Time Workshop. The displacement measurements were supplied to dSpace system where control signal was obtained from CC algorithm. The signal was amplified and supplied to the control winding.

## RESULTS

In the identification, band-limited (500 Hz) white noise voltage supply to the control winding was used. The displacement was measured and frequency responses processed. The frequency response from the

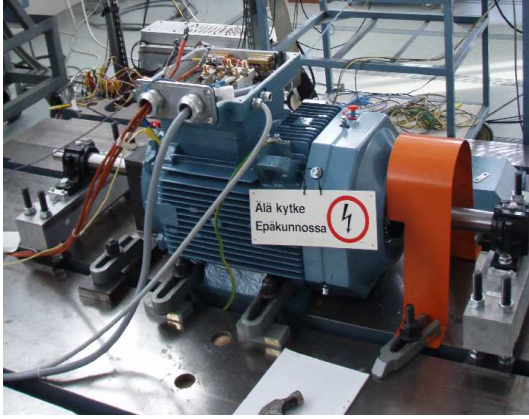


**Figure 1:** The test machine used in experiments.

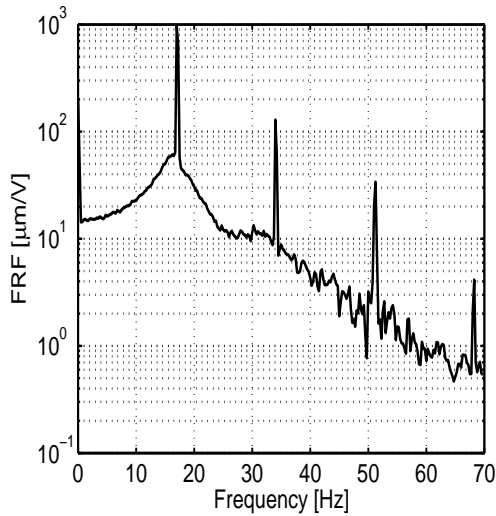


**Figure 2:** Frequency response of the actuator-rotor system.

voltage input to the displacement output is shown in Fig. 2.

In Fig. 3 the rotor orbit is shown when control winding was not excited ( $\hat{U}_{c,2} = 0$ ). Current is induced in the control winding due to the eccentric rotor motion which produces a four-pole flux in the air-gap. In Fig. 4, the current in the control winding is shown.

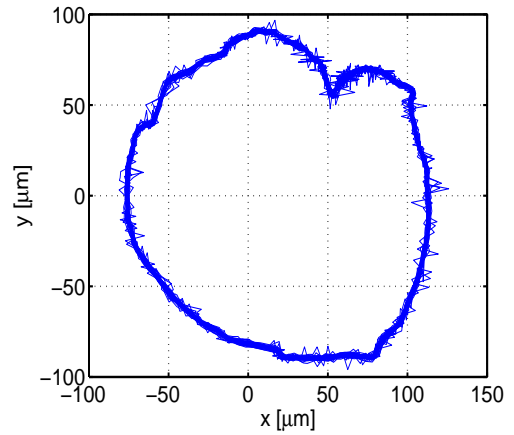


**Figure 3:** Rotor orbit when control winding was not excited ( $\hat{U}_c = 0$ ).

The identification of the actuator-rotor system was performed in the frequency domain by using the frequency responses (see Fig. 2) and curve fitting. As a result, the transfer function  $\mathcal{H}(j\omega)$  in Eq. (8) was estimated for frequencies  $\omega = 0, \omega_m, 2\omega_m, 3\omega_m$ . The CC algorithm was hence employed by including these four harmonics. The higher harmonics had a minor influence on the rotor vibration amplitudes, and hence, only the first four harmonics were included.

With CC algorithm, in Eq. (8), the convergence coefficients  $\gamma = 1$ ,  $\alpha_0 = 5 \cdot 10^{-5}$ ,  $\alpha_1 = 2 \cdot 10^{-4}$  and  $\alpha_2 = \alpha_3 = 10^{-4}$  were used. In Fig. 5, the horizontal rotor displacement is shown when CC control was switched on. For the Fourier coefficient calculation in Eq. (8) instantaneous coefficient update [8, 9] was applied. The vibration amplitudes reduce 85%. This is due to the compensation of the rotor rotation harmonic components. Indeed, in Fig. 6 spectrum of the horizontal rotor displacement is shown with and with-

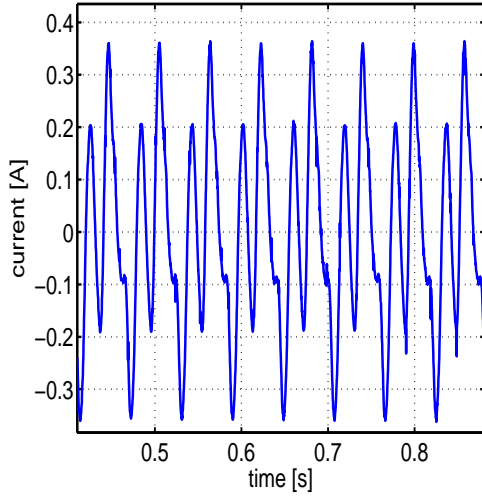


**Figure 4:** Current in a single control winding phase induced by eccentric rotor motion ( $\hat{U}_c = 0$ ).

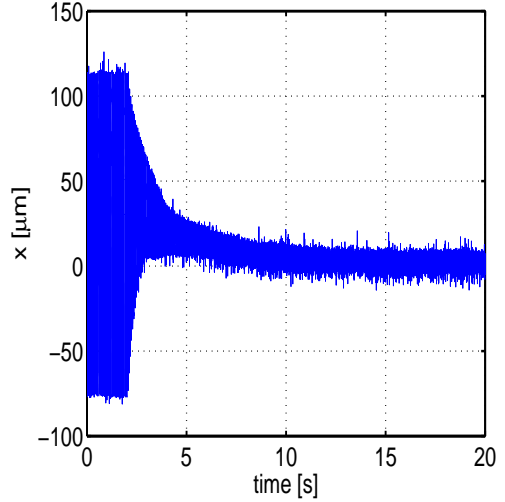


**Figure 5:** Horizontal rotor displacement when CC - algorithm is switched on.

out the control applied. Results show that the first four harmonics included in the CC algorithm reduce noticeably. As well, as can be seen from Fig. 5, the vibration control centralizes the rotor originally not whirling around the stator bore center. The centralizing is caused by the zero-harmonic ( $\omega_0$ ) CC-control.

In Fig. 7 the voltage supplied to the control winding when CC algorithm has converged to its stationary operation is shown.

## DISCUSSION AND CONCLUSIONS

In this paper, flexural rotor vibration in a two-pole cage induction machine equipped with a supplementary winding based on self-bearing technology was considered. A low-order parametric model was deduced for the actuator-rotor system under eccentric rotor motion.

The actuator-rotor system was identified in the frequency domain by using measurement data of a small two-pole cage induction motor. Based on the identification, an adaptive control algorithm was used for attenuation of rotor rotation harmonic vibration components. The results show that a considerable level

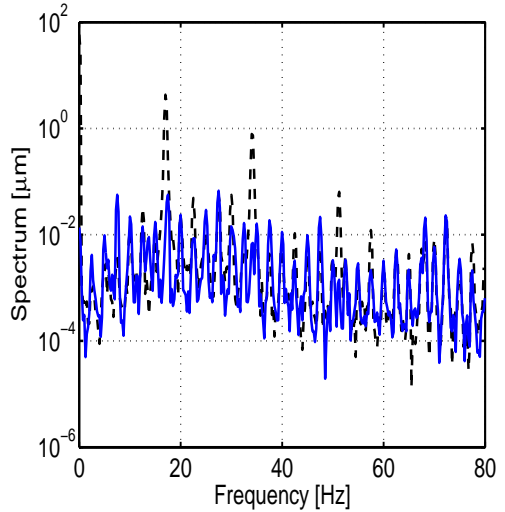


**Figure 6:** Spectrum of the horizontal rotor displacement. Without control (dashed line) and with CC control (solid line).

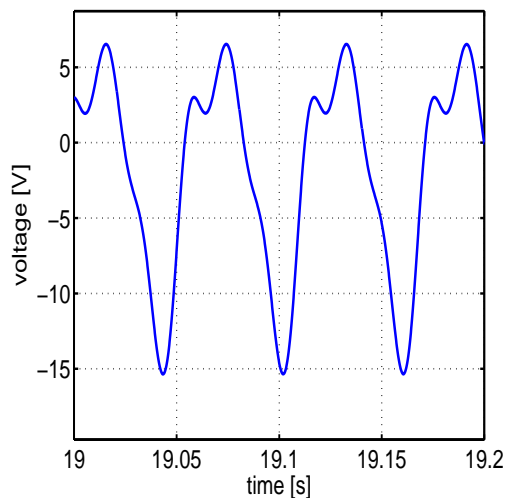


**Figure 7:** Voltage  $\text{Re}(\hat{U}_c)$  supplied to the control winding.

of flexural rotor vibration suppression (85% reduction in amplitude) can be achieved by compensating low-order dominant vibration components.

The built-in force actuator provides means of producing a controlled force on the rotor. In this paper, the force actuator was applied for vibration attenuation and its efficiency was shown. The built-in force actuator may also be used for condition monitoring or fault diagnostics: i) the machine can be excited with the actuator and the responses monitored, ii) the currents induced in the control winding can be used as signatures of possible faults, iii) control commands may be monitored as indicators of changes in machine state, analogically to the methodology used in active magnetic bearings.

## ACKNOWLEDGEMENTS

The authors gratefully acknowledge financial support from the Academy of Finland and VTT Technical Research Center of Finland. Special thanks are devoted to Prof. Marko Hinkkanen, Helsinki University of Technology, Power Electronics Laboratory, for guidance with the dSpace system.

## REFERENCES

- [1] A. Smith, D. Dorrell, Calculation and measurement of unbalanced magnetic pull in cage induction motors with eccentric rotors. part i: Analytical model, *Proc. IEE Electric Power Applications* 143(3) (1996) 193–201.
- [2] A. Chiba, D. T. Power, M. A. Rahman, Characteristics of a bearingless induction motor, *IEEE Trans. Magn.* 27(6) (1991) 5199–5201.
- [3] A. Chiba, T. Fukao, M. Rahman, Vibration suppression of a flexible shaft with a simplified bearingless induction motor drive, *Conference Record of the 2006 IEEE Industry Applications Conference 2006. 41st IAS Annual Meeting. vol.2* (2006) 836–842.
- [4] T. P. Holopainen, A. Tenhunen, E. Lantto, A. Arkkio, Unbalanced magnetic pull induced by arbitrary eccentric motion of cage rotor in transient operation, part 1: Analytical model, *Electrical Engineering (Archiv für Electrotechnik)* 88(1) (2005) 13–24.
- [5] A. Laiho, K. Tammi, K. Zenger, A. Arkkio, A model-based flexural rotor vibration control in cage induction electrical machines by a built-in force actuator, *Electrical Engineering (Archiv für Electrotechnik)* 90(6) (2008) 407–421.
- [6] C. Knospe, S. Fedigan, R. W. Hope, R. Williams, A multitasking dsp implementation of adaptive magnetic bearing control, *IEEE Transactions on Control Systems Technology* 5(2) (1997) 230–238.
- [7] P. K. Kovács, *Transient phenomena in electrical machines*, Elsevier Science Publishers, Amsterdam, 1984.
- [8] S. Daley, J. Hätönen, K. Tammi, Instantaneous harmonic vibration control of a flexible rotor, *Proceedings of the International Symposium on Active Control of Sound and Vibration, Adelaide, Australia, 18 - 20 Sept. 2006* (2006) 11p.

- [9] K. Tammi, Active control of radial rotor vibrations: Identification, feedback, feed-forward, and repetitive control methods, Doctoral dissertation, Helsinki University of Technology, Department of Automation and Systems Technology (2007) 1–165, <http://lib.tkk.fi/Diss/2007/isbn9789513870089/>.